Electronic Supplementary Material (ESI) for Dalton Transactions.
This journal is © The Royal Society of Chemistry 2020

Supporting Information

Incorporation of a Nitrogen-Rich Energetic Ligand in a $\{Yb^{III}_2\}$ Complex Exhibiting Slow Relaxation of the Magnetisation Under an Applied Field

Paul Richardson,[a] Diogo Alves Gálico,[a] Jeffrey Ovens,[a] Fernando A. Sigoli[b] and Muralee Murugesu[a]*

[a.] *Department of Chemistry and Biomolecular Sciences, University of Ottawa, ON, Canada, K1N 6N5. Email: m.murugesu@uottawa.ca; Fax: +1 (613) 562 5170; Tel: +1 (613) 562 5800 ext. 2733*

[b.] *Institute of Chemistry, University of Campinas, UNICAMP, P.O. Box 6154, Campinas, São Paulo, 13083-970, Brazil*

Experimental Details

Materials

$Yb(fod)_3$ was purchased from Strem Chemicals and used without further purification or synthesized utilizing a previously reported procedure.[1] 3,6-dihydrazinyl-1,2,4,5-tetrazine was synthesized according to a previously reported procedure.[2] Reactions for the synthesis of **1** was performed under anaerobic conditions in a nitrogen-filled glovebox. Acetonitrile (MeCN), which was of reagent grade, was dried on columns of activated alumina utilizing a J.C. Meyer solvent purification system and degassed using multiple freeze-pump-thaw cycles. The dried and degassed solvent was stored over 3Å molecular sieves. The synthesized hydrated salt of $Yb(fod)_3$ was subsequently dried and purified using vacuum sublimation with a water-cooled cold finger at a temperature of approximately 100 °C.

Synthesis

$[Yb_2(dhtz)(fod)_6]\cdot 2MeCN$ (1). To a brown suspension of dhtz (0.375 mmol, 53 mg) in MeCN (10 mL), was added anhydrous $Yb(fod)_3$ (0.125 mmol, 132 mg). The reaction mixture was stirred for 15 minutes, over which time the reaction mixture went from a brown suspension to an orange solution with brown particulate. The reaction mixture was then filtered through a fine glass frit to remove the brown particulate, which was unreacted dhtz. The now clear orange solution was placed in a -35 °C freezer in the glovebox overnight, upon which orange block crystals were obtained. The isolated crystals were found to be air and moisture stable based on initial $Yb(fod)_3$ used. Yield = 18 %. Elemental analysis (%). Calculated: C, 32.96; H, 2.94; N, 4.96. Found: C, 32.64; H, 2.49; N, 4.95. IR (ATR, cm^{-1}): 2972 (w), 1621 (s), 1508 (s), 1349 (m), 1208 (s, broad), 1152 (s, broad), 1066 (m), 967 (s), 941 (m), 913 (m), 834 (w), 794 (m), 754 (w), 694 (m), 591 (w)

Physical Characterization

Infrared analysis was performed with a Nicolet 6700 FT-IR spectrometer equipped with an ATR from 4000 – 500 cm^{-1}. Elemental analysis was performed using a vario Isotope Cube equipped with an autosampler.

Magnetic Characterization

Magnetic measurements were performed using a Quantum Design MPMS-XL7 SQUID magnetometer, with an operating range of 300 – 1.8 K for applied dc fields of -7 to 7 T. An *M* vs. *H* measurement was performed at 100 K as an impurity check, and no ferromagnetic impurities were found in the sample. Direct current (dc) susceptibility measurements were performed on a freshly filtered crushed polycrystalline sample of **1** (23.4 mg) and was sealed in a polypropylene bag (23.2 mg) at applied field of 1000 Oe. Magnetisation versus field (*M* vs. *H*) measurements were performed from 1.9 to 7 K and from 0 to 7 T. Alternating current (ac) magnetic susceptibility studies were performed under an oscillating ac field of 3.78 Oe and frequencies ranging from 0.1 to 1500 Hz. Field-dependent ac measurements were performed at a constant temperature of 2 K, and frequency-dependent ac measurements were performed at a constant applied dc field of 900 Oe. All magnetic data was corrected for the diamagnetic contributions of the sample holder, polypropylene bag, and intrinsic contributions from the sample utilizing Pascal's constants.

Optical Characterization

Photoluminescence measurements were performed using a Fluorolog-3 spectrofluorometer (Horiba FL3-22-iHR320). An ozone-free Xenon lamp of 450 W (Ushio) was used as a radiation source. The emission spectra were recorded using an iHR320 emission monochromator and a Hamamatsu H10330A-75 photomultiplier. The sample was placed inside a Janis VNF-100 cryostat controlled by a Cryocon 32B temperature controller.

Single Crystal X-Ray Diffraction

Crystallographic data were collected by the X-Ray Core Facility at the University of Ottawa. A single crystal of compound **1** was mounted on a MiTeGen MicroMount using Parabar oil. X-ray diffraction data were collected at 200(2) K with a Bruker Kappa ApexII diffractometer equipped with a Mo Kα ($\lambda = 0.71073$ Å) sealed-tube source, an ApexII CCD detector and a refrigerated compressed air sample cooling system. Raw data processing, including integration, absorption corrections, and determination of the space group through systematic absences was performed using the Apex3 software suite from Bruker.[3] The initial structural solution was determined using charge flipping methods via Superflip,[4] and subsequent refinements were made based on F^2 using Crystals[5] software. The "soft" nature of the packing resulted in a poorly defined configuration for the fod^- groups and an excess of positional and configurational disorder. Therefore, all 1,2 and 1,3 distance and 1,2 vibrational restraints were applied within the fod^- groups (no restraints were used for Yb-O or Yb-N distances or angles). These restraints were also used on the free MeCN solvent molecules, and some 1,2 vibrational restraints were used within the bridging dhtz ligand. Hydrogen atoms were placed geometrically and refined using a riding model.

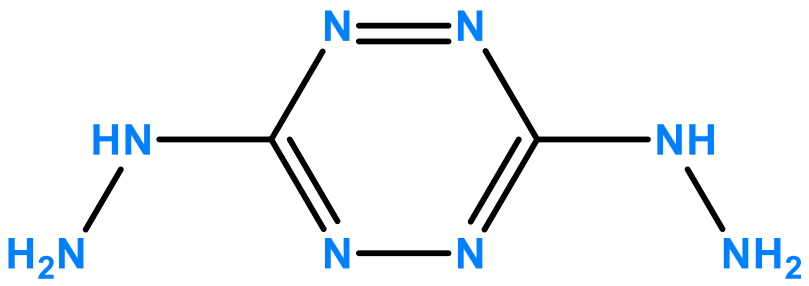

Scheme S1 Structure of 3,6-dihydrazinyl-1,2,4,5-tetrazine (dhtz).

Table S1 Crystallographic data for compound **1**.

Compound	**1**
Empirical formula	$C_{62}H_{66}F_{42}N_8O_{12}Yb_2 \cdot 2(C_2H_3N)$
Crystal system	Monoclinic
Space group	$P2_1/n$
a (Å)	14.55590(4)
b (Å)	18.25540(4)
c (Å)	17.91350(4)
α (°)	90
β (°)	103.150(4)
γ (°)	90
V (Å^3)	4635.22(8)
Z	2
ρ_{calc} (g cm^{-3})	1.677
λ (Å)	0.71073
T (K)	200(2)
μ (mm^{-1})	2.147
F (000)	2304
Reflections collected	29676
Independent reflections	8369
Reflections with $I > 2\sigma(I)$	4867
Goodness of fit on F^2	0.8545
R_1, wR_2 ($I > 2\sigma(I)$)[a]	0.1036, 0.0651
R_1, wR_2 (all data)	0.1469, 0.0679
Data/Parameter Ratio	10.46

Table S2. Selected bond distances of **1**.

Bond	Distance (Å)	Bond	Distance (Å)
Yb1 – N1	2.520	Yb1 – O3	2.195
Yb1 – N3	2.402	Yb1 – O4	2.239
Yb1 – O1	2.162	Yb1 – O5	2.235
Yb1 – O2	2.295	Yb1 – O6	2.239

Table S3. Selected bond angles of **1**.

Bonds	Angle (°)	Bonds	Angle (°)
N1 – Yb1 – N3	63.94	O3 – Yb1 – O4	74.31
O1 – Yb1 – O2	74.37	O5 – Yb1 – O6	72.44

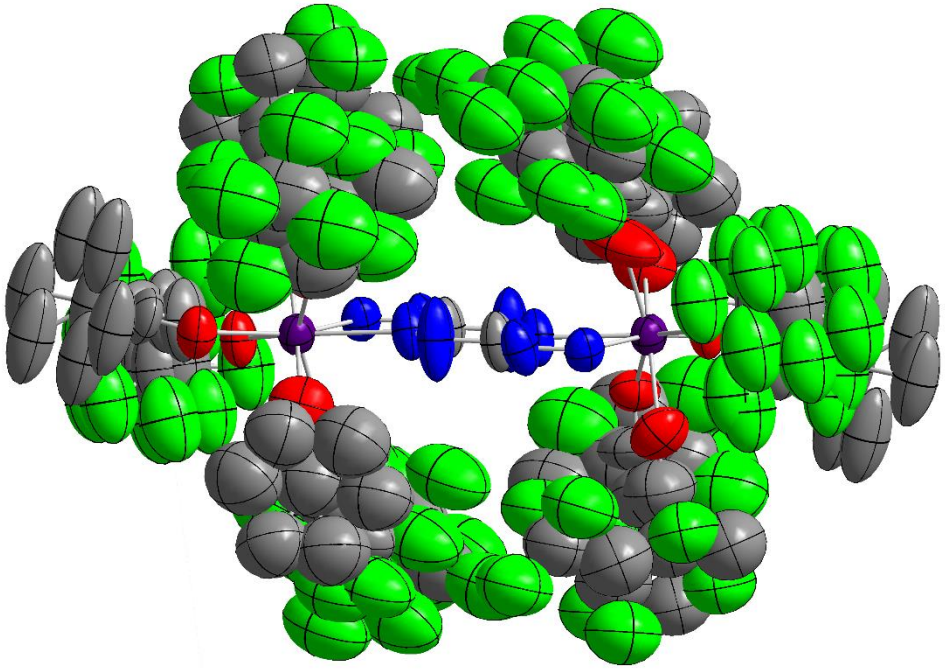

Figure S1. Thermal ellipsoid depiction of compound **1**. Solvent molecules and H atoms have been omitted for clarity. Colour scheme: Yb, purple; O, red; N, blue; C, grey.

Table S4. SHAPE Analysis of Yb1 metal centre in **1**.

Geometry (SHAPE Code)	CShM for Yb1
Octagon (OP-8)	29.418
Heptagonal pyramid (HPY-8)	23.816
Hexagonal bipyramid (HBPY-8)	15.568
Cube (CU-8)	11.321
Square antiprism (SAPR-8)	**1.407**
Triangular dodecahedron (TDD-8)	**1.385**
Johnson gyrobifastigium J26 (JGBF-8)	12.600
Johnson elongated triangular bipyramid J14 (JETBPY-8)	27.363
Biaugmented trigonal prism J50 (JBTPR-8)	1.588
Biaugmented trigonal prism (BTPR-8)	**1.384**
Snub diphenoid J84 (JSD-8)	3.167
Triakis tetrahedron (TT-8)	11.886
Elongated trigonal bipyramid (ETBPY-8)	23.837

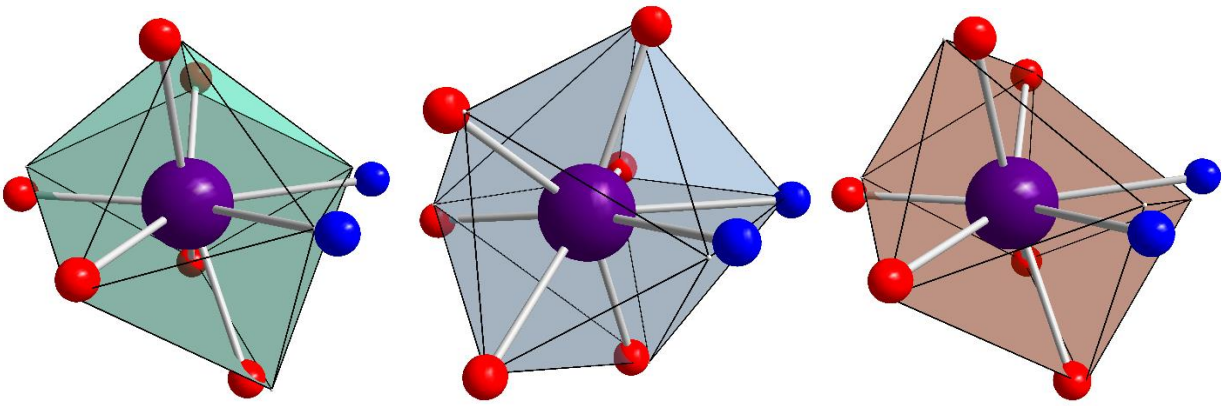

Figure S2. Coordination environment of Yb1 metal centre in **1**. The polyhedra represent the ideal geometries as determined by SHAPE (BTPR, pale green; TDD, blue; SAPR, orange). Colour code: Yb, purple; O, red; N, blue.

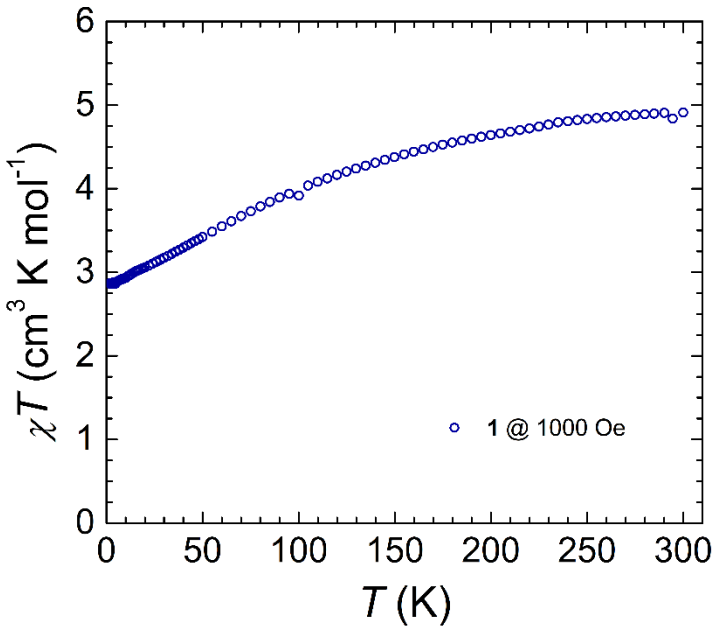

Figure S3. Solid-state temperature dependence of the χT product under 0.1 T for compound **1**, with χ being the molar susceptibility per dinuclear complex defined as M/H.

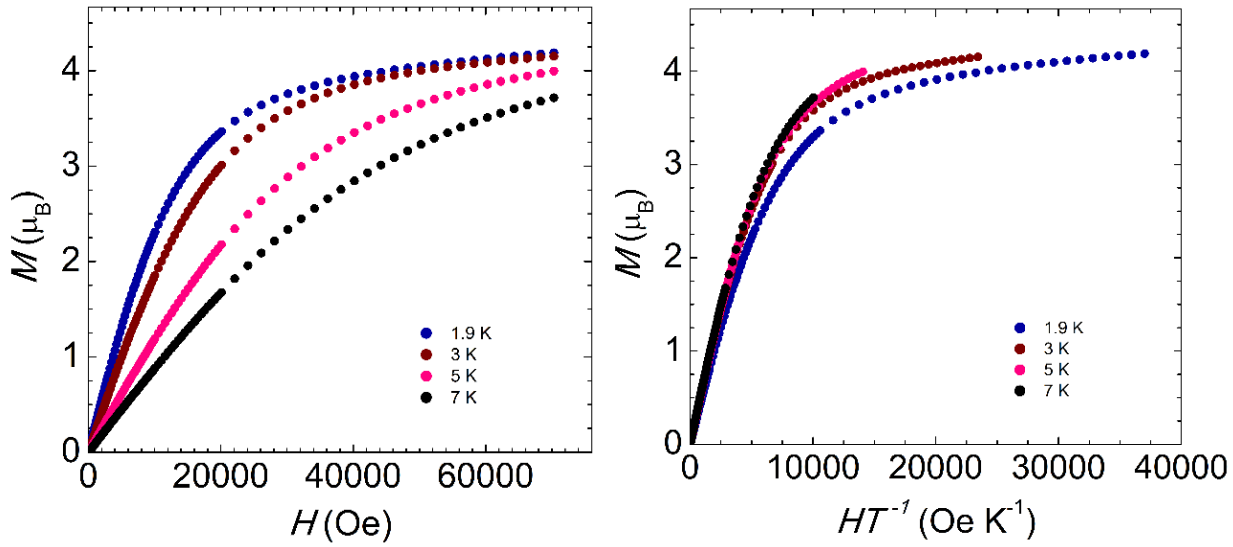

Figure S4. Solid state field dependence of the magnetization (left) and reduced magnetization (right) for **1** at the indicated temperatures.

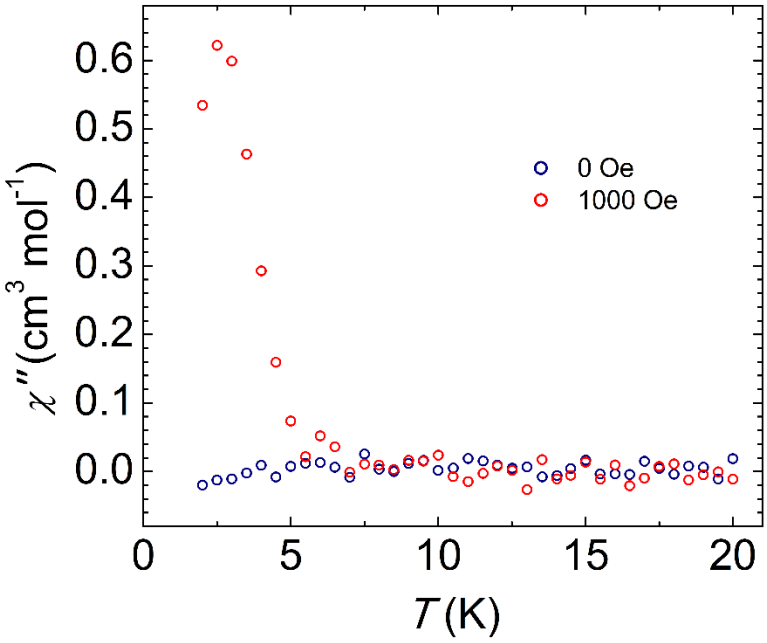

Figure S5. χ'' ac magnetic susceptibility checks at both 0 Oe and 1000 Oe for compound **1** performed from 20 to 2 K. No peak is observed over the given temperature range at zero field.

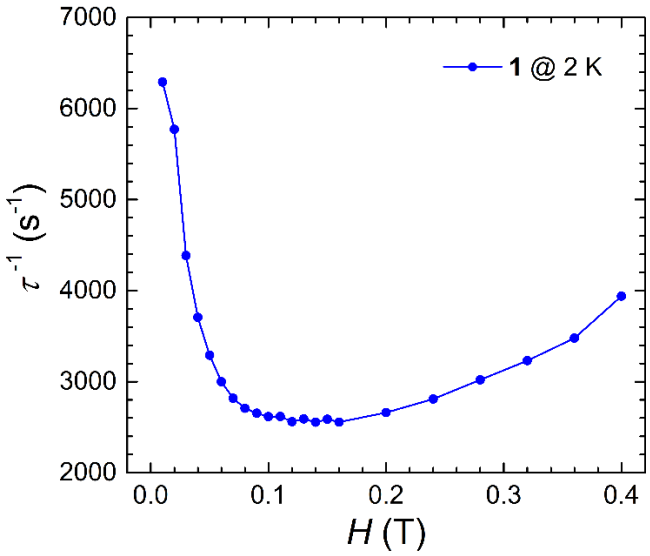

Figure S6. The characteristic frequency of the high-frequency process for **1**, obtained at 2 K. Values of τ^{-1} were obtained using a generalized or double Debye model where appropriate. The line is a guide for the eye.

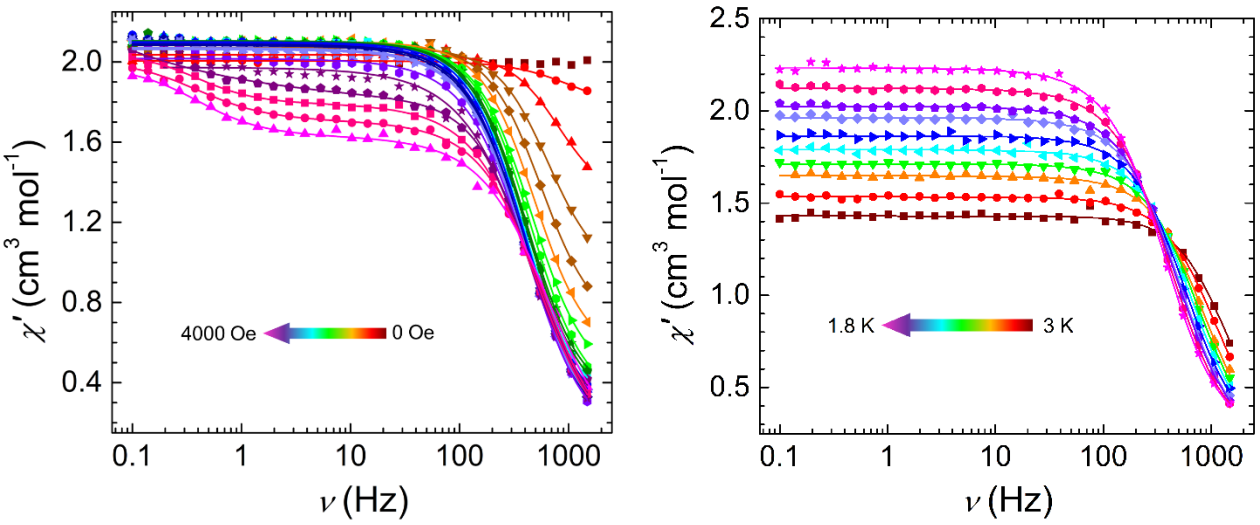

Figure S7. Field-dependence (left) and frequency-dependence (right) of the χ' ac magnetic susceptibility of **1**. Field-dependent studies were performed at 2 K, and frequency-dependent studies were performed at 900 Oe. Curves are lines of best fit of a generalized or double Debye model.

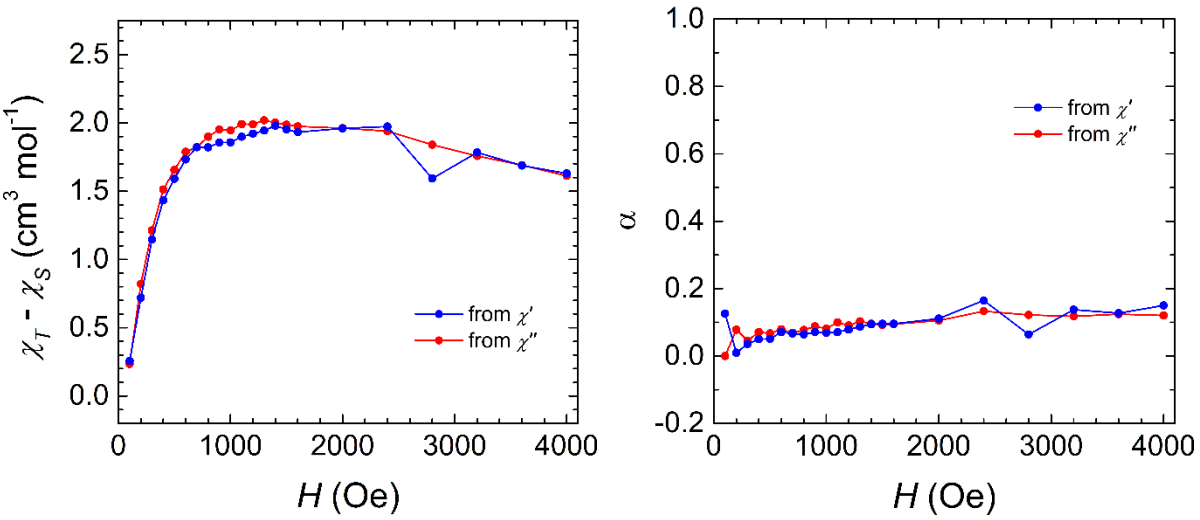

Figure S8. Data obtained from the Debye fits of the χ' and χ'' frequency-dependent ac data collected at a constant temperature of 2 K for compound **1**. χ_T - χ_S (left) and α (right) comparisons. Data should overlap as closely as possible.

Table S5. Extracted values of χ_S, χ_T, α, and τ from fitting the field-dependent χ' magnetic susceptibility data, either through a generalized Debye or double Debye model where necessary.

H (Oe)	τ (High Frequency Process)	τ (Low Frequency Process)	α (High Frequency Process)	α (Low Frequency Process)	χ_S (High Frequency Process)	χ_S (Low Frequency Process)	χ_T (High Frequency Process)	χ_T (Low Frequency Process)
0	-	-	-	-	-	-	-	-
100	1.43E-04	-	0.12589	-	1.7504	-	2.00583	-
200	1.96E-04	-	0.00947	-	1.31679	-	2.03579	-
300	2.45E-04	-	0.03563	-	0.92529	-	2.07164	-
400	2.83E-04	-	0.05011	-	0.65841	-	2.09072	-
500	3.25E-04	-	0.05092	-	0.51301	-	2.10329	-
600	3.46E-04	-	0.07093	-	0.37341	-	2.1056	-
700	3.57E-04	-	0.06656	-	0.28297	-	2.10501	-
800	3.86E-04	-	0.06412	-	0.28438	-	2.10542	-
900	3.90E-04	-	0.07039	-	0.24945	-	2.10511	-
1000	4.06E-04	-	0.06819	-	0.24091	-	2.09792	-
1100	4.06E-04	-	0.07056	-	0.2015	-	2.09979	-
1200	4.12E-04	-	0.07882	-	0.17293	-	2.09362	-
1300	4.04E-04	-	0.08686	-	0.14551	-	2.08927	-
1400	3.97E-04	-	0.0942	-	0.10284	-	2.08296	-
1500	4.03E-04	-	0.09557	-	0.11866	-	2.07071	-
1600	4.06E-04	-	0.09545	-	0.13005	-	2.06261	-
2000	3.82E-04	-	0.11106	-	0.05725	-	2.01703	-
2400	3.47E-04	-	0.16499	-	1.00E-05	-	1.97338	-
2800	3.71E-04	209.588	0.06379	0.63661	0.20213	1.00E-07	1.79505	2
3200	3.10E-04	0.40358	0.13731	0.09352	0.01	8.03E-04	1.7932	0.25145
3600	2.77E-04	0.40189	0.12691	0.17333	0.01786	6.47E-04	1.70543	0.3093
4000	2.45E-04	0.39943	0.15006	0.14109	1.00E-05	0	1.62985	0.3517

Table S6. Extracted values of χ_S, χ_T, α, and τ from fitting the field-dependent χ'' magnetic susceptibility data, either through a generalized Debye or double Debye model where necessary.

H (Oe)	*τ* (High Frequency Process)	*τ* (Low Frequency Process)	*α* (High Frequency Process)	*α* (Low Frequency Process)	χ_S (High Frequency Process)	χ_S (Low Frequency Process)	χ_T (High Frequency Process)	χ_T (Low Frequency Process)
0	-	-	-	-	-	-	-	-
100	1.59E-04	-	9.32E-16	-	1.00154	-	0.76741	-
200	1.73E-04	-	0.07781	-	0.82478	-	0.00293	-
300	2.28E-04	-	0.04581	-	1.34671	-	0.13425	-
400	2.70E-04	-	0.07091	-	1.51315	-	0.00144	-
500	3.04E-04	-	0.06736	-	1.65775	-	0.00102	-
600	3.33E-04	-	0.07921	-	1.789	-	0.00128	-
700	3.55E-04	-	0.06886	-	1.82381	-	0.00106	-
800	3.69E-04	-	0.07735	-	1.90008	-	0.00178	-
900	3.77E-04	-	0.08793	-	1.95498	-	0.00224	-
1000	3.82E-04	-	0.0814	-	1.9683	-	0.02351	-
1100	3.82E-04	-	0.09977	-	1.99448	-	0.00348	-
1200	3.91E-04	-	0.09044	-	2.00121	-	0.01129	-
1300	3.86E-04	-	0.10282	-	2.03855	-	0.01916	-
1400	3.91E-04	-	0.09566	-	2.00737	-	0.00602	-
1500	3.86E-04	-	0.09245	-	1.98853	-	0.00247	-
1600	3.91E-04	-	0.09478	-	1.97644	-	0.00198	-
2000	3.76E-04	-	0.10509	-	1.96295	-	0.00115	-
2400	3.56E-04	-	0.13312	-	1.94122	-	0.0019	-
2800	3.31E-04	0.3408	0.12167	0.09322	1.84047	0.18021	4.08E-04	9.51E-04
3200	3.10E-04	0.32452	0.11793	0.09876	1.78516	0.22713	0.0275	9.42E-04
3600	2.87E-04	0.3604	0.12418	0.11755	1.71158	0.2804	0.02173	8.25E-04
4000	2.54E-04	0.36829	0.12032	0.12559	1.64555	0.32741	0.03344	5.63E-04

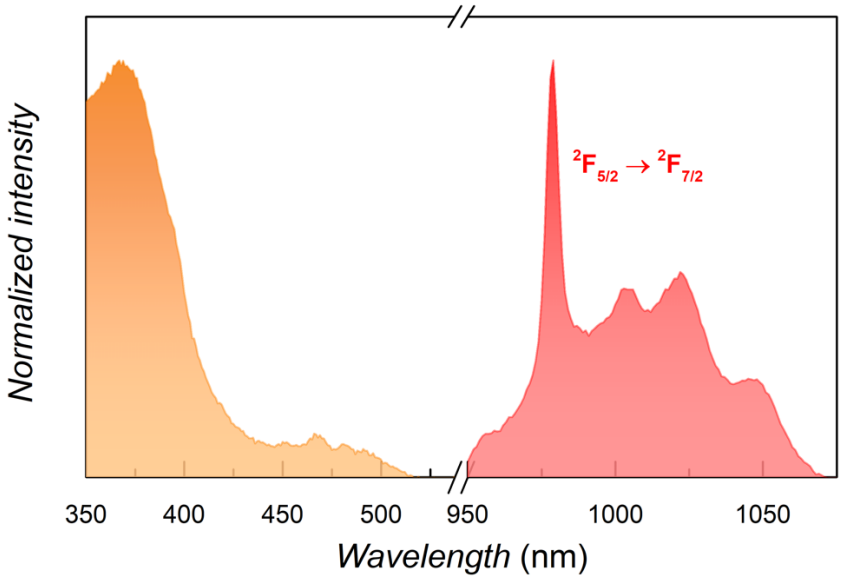

Figure S9. Excitation (λ_{em} = 978 nm, left) and emission (λ_{ex} = 368 nm, right) spectra of compound **1** obtained at room temperature. Large component in the excitation due to fod^- co-ligands while the lower component between 430 – 520 cm^{-1} is due to dhtz ligand.

Table S7. Energies of the m_J sublevels of the ground ($^2F_{5/2}$) and excited ($^2F_{7/2}$) levels obtained *via* photoluminescence spectroscopy. The errors on this measurement are ± 10 cm^{-1}.

Level	Energy (cm^{-1})
$^2F_{7/2}$	0
	240
	424
	644
$^2F_{5/2}$	10220
	10280
	-

References

1. C. S. Springer Jr., D. W. Meek and R. E. Sievers, *Inorg. Chem.*, **1967**, 6, 1105.
2. B. Venkateswara Rao, S. Dhokale, P. R. Rajamohanan and S. Hotha, *Chem. Commun.*, **2013**, 49, 10808.
3. APEX Software Suite v 2010 Bruker AXS Inc. Madison Wisconsin USA, 2010.
4. G. Oszlanyi and A. Suto, *Acta Crystallogr. A*, **2004**, 60, 134.
5. P. W. Betteridge, J. R. Carruthers, R. I. Cooper, K. Prout and D. J. Watkin, *J. Apply. Cryst.*, **2003**, 36, 1487.